RESEARCH ARTICLE

Dynamics of intraoceanic subduction initiation: 1. Oceanic detachment fault inversion and the formation of supra-subduction zone ophiolites

Marco Maffione[1], Cedric Thieulot[1,2], Douwe J. J. van Hinsbergen[1], Antony Morris[3], Oliver Plümper[1], and Wim Spakman[1,2]

[1]Department of Earth Sciences, University of Utrecht, Utrecht, Netherlands, [2]Centre for Earth Evolution and Dynamics, Oslo, Norway, [3]School of Geography, Earth and Environmental Sciences, Plymouth University, Drake Circus, Plymouth, UK

Abstract Subduction initiation is a critical link in the plate tectonic cycle. Intraoceanic subduction zones can form along transform faults and fracture zones, but how subduction nucleates parallel to mid-ocean ridges, as in e.g., the Neotethys Ocean during the Jurassic, remains a matter of debate. In recent years, extensional detachment faults have been widely documented adjacent to slow-spreading and ultraslow-spreading ridges where they cut across the oceanic lithosphere. These structures are extremely weak due to widespread occurrence of serpentine and talc resulting from hydrothermal alteration, and can therefore effectively localize deformation. Here, we show geochemical, tectonic, and paleomagnetic evidence from the Jurassic ophiolites of Albania and Greece for a subduction zone formed in the western Neotethys parallel to a spreading ridge along an oceanic detachment fault. With 2-D numerical modeling exploring the evolution of a detachment-ridge system experiencing compression, we show that serpentinized detachments are always weaker than spreading ridges. We conclude that, owing to their extreme weakness, oceanic detachments can effectively localize deformation under perpendicular far-field forcing, providing ideal conditions to nucleate new subduction zones parallel and close to (or at) spreading ridges. Direct implication of this, is that resumed magmatic activity in the forearc during subduction initiation can yield widespread accretion of suprasubduction zone ophiolites at or close to the paleoridge. Our new model casts the enigmatic origin of regionally extensive ophiolite belts in a novel geodynamic context, and calls for future research on three-dimensional modeling of subduction initiation and how upper plate extension is associated with that.

1. Introduction

Subduction initiation refers to the time interval when oceanic lithosphere first descends into the upper mantle before the onset of self-sustaining subduction [*Gurnis et al.*, 2004]. It is an episodic process currently occurring at a few localities on Earth [*Gurnis et al.*, 2004]. Disagreement on the driving mechanism(s) and kinematics of subduction initiation have culminated in two contrasting models, with subduction initiating by either (i) spontaneous sinking of old lithosphere that is denser than the underlying mantle at transform faults and fracture zones [*Stern*, 2004], or (ii) far-field forces overcoming both frictional resistance at preexisting faults and the lithosphere's resistance to bending [*Gurnis et al.*, 2004]. Although existing models may explain subduction initiation along transform faults and fracture zones [e.g., *Toth and Gurnis*, 1998; *Hall et al.*, 2003; *Gurnis et al.*, 2004; *Leng and Gurnis*, 2011], they fail to explain subduction nucleating parallel to spreading ridges. In fact, spontaneous gravitational collapse of spreading ridges is unlikely given their buoyancy, and numerical modeling of forced subduction initiation at a ridge (in the absence of any other lithospheric weakness zone) showed that this process requires extremely large external forces to be accomplished [*Gurnis et al.*, 2004]. However, thousands of kilometers long intraoceanic subduction zones formed in the Neotethys during the Late Jurassic and Late Cretaceous in response to convergence that was at high angles to passive margins of Laurasia and Gondwana (i.e., Africa, Arabia, and India) [e.g., *Agard et al.*, 2007]. Since spreading ridges are commonly parallel (or at low-angle) to passive margins, we infer that at least part of the Neotethyan subduction zones must have formed (sub)parallel to ridges, rather than transform faults or fracture zones. Ridge-parallel intraoceanic subduction zones were, in particular, proposed to have formed during the Jurassic in the western Neotethys, relics of which are preserved in the geological

record of the Dinaric-Hellenic belt of Albania and Greece in the Balkan Peninsula [e.g., *Bortolotti et al.*, 2002; *Schmid et al.*, 2008; *Robertson*, 2012; *Bortolotti et al.*, 2013].

Not only it is difficult to envisage how subduction would start at a mid-oceanic ridge, but also the study of ophiolites, which are exposed remnants of oceanic lithosphere, provides an additional complexity. Regionally extensive ophiolite belts were derived from leading edges (forearcs) of oceanic upper plates that became emergent due to underthrusting of continental margins [e.g., *Dewey*, 1976; *Moores*, 1982; *Casey and Dewey*, 1984]. The majority of these ophiolites have a so-called suprasubduction zone (SSZ) geochemical signature that resulted from remelting of a mantle source that had already been depleted by mid-ocean ridge basalt (MORB) extraction, due to the addition of slab-derived fluids [e.g., *Pearce et al.*, 1984]. SSZ ophiolites are thought to form at spreading centers in a forearc during the subduction initiation process [*Stern and Bloomer*, 1992; *Shervais*, 2001; *Stern*, 2004; *Stern et al.*, 2012]. Proposed driving mechanisms for the formation of forearc ophiolites include: (i) melting of the upwelling mantle filling the gap in the forearc that would arise from spontaneous sinking of the lithosphere at transform faults [*Stern*, 2004], (ii) magmatic activity at a stretching upper plate due to slab foundering and initial roll-back after forced subduction initiation at a fracture zone or transform fault [*Hall et al.*, 2003; *Leng and Gurnis*, 2011; *Leng et al.*, 2012], or (iii) sustained magmatic activity at a preexisting spreading center during subduction initiation along a transform fault [*Dewey and Casey*, 2011]. It still remains, however, hard to explain how long ophiolite belts could develop in a forearc during subduction initiation parallel and close to (or at) a preexisting spreading ridge.

In this paper, we present geochemical, structural geological, and paleomagnetic evidence from the ophiolites of Albania and Greece assessing whether intraoceanic subduction formed in the western Neotethys Ocean in the Jurassic parallel to but not at the ridge axis. We will develop our results in a geodynamic model, assisted by numerical experiments, testing which weakness zones found in modern slow-spreading mid-ocean ridges may play a role in localizing strain if a young ridge would be imposed to contraction, and place this in ongoing discussion about the formation of SSZ ophiolites.

2. Slow-Spreading Ridges and Oceanic Detachment Faults

Deep oceanic exploration has documented that in slow-spreading and ultraslow-spreading systems plate divergence is not, or episodically accommodated by magmatic accretion, but instead by low-angle, large-offset extensional detachment faults [e.g., *Cannat et al.*, 1995; *Cann et al.*, 1997; *Blackman et al.*, 1998, 2011; *Tucholke et al.*, 1998; *MacLeod et al.*, 2002, 2009; *Dick et al.*, 2003; *Smith et al.*, 2006, 2008, 2014; *Ildefonse et al.*, 2007; *Escartín et al.*, 2008a]. Flexural bending of detachment footwalls results in rotated dome-shaped structures (oceanic core complexes) that expose lower crustal and upper mantle rocks [*Garcés and Gee*, 2007; *Smith et al.*, 2008; *Morris et al.*, 2009; *MacLeod et al.*, 2011; *Sauter et al.*, 2013; *Whitney et al.*, 2013]. Detachments are usually symmetric to and dip toward spreading axes [*MacLeod et al.*, 2009; *Reston and Ranero*, 2011] and typically form at or near and parallel to the axis [*Smith et al.*, 2006, 2008; *Escartín et al.*, 2008a]. Older detachments are observed to be preserved off-axis during spreading [*Smith et al.*, 2006, 2008; *Reston and Ranero*, 2011]. Detachment faults pervasively cut the lithosphere to depths of ~7 km [*Escartín et al.*, 2008a; *Reston and Ranero*, 2011], providing pathways for seawater to infiltrate the lower crust and upper mantle and trigger pervasive hydrothermal alteration (serpentinization) [e.g., *Schroeder et al.*, 2002; *Mével*, 2003; *Bach et al.*, 2004, 2006; *Boschi et al.*, 2006a, 2013; *Beard et al.*, 2009; *Klein et al.*, 2009; *Plümper et al.*, 2012, 2014; *Andreani et al.*, 2014; *Maffione et al.*, 2014]. As a result, detachments are associated with a relatively thick (up to 200 m) crystal-plastic (mylonitic) to cataclastic shear zone dominated by serpentine minerals and other phyllosilicates, including talc and chlorite [*MacLeod et al.*, 2002; *Escartín et al.*, 2003; *Schroeder and John*, 2004; *Boschi et al.*, 2006a, 2006b; *Karson et al.*, 2006; *Escartín et al.*, 2008b; *Andreani et al.*, 2014]. Serpentinization likely affects also deeper portions of the fault footwall, and may produce an even thicker (up to 2 km) alteration zone below the detachment fault surface [*Escartín et al.*, 2003; *Schroeder and John*, 2004; *Boschi et al.*, 2006a; *Maffione et al.*, 2014].

Serpentine minerals are stable between 200 and 500°C at pressures < 4 GPa, have a low viscosity (~10^{18}–10^{19} Pa.s) [e.g., *Hilairet et al.*, 2007] and friction coefficient ($\mu = 0.15$–0.45) [*Escartín et al.*, 1997], and has a strength that is at least an order of magnitude lower than that of unaltered mantle or crustal rocks [*Escartín et al.*, 1997; *MacLeod et al.*, 2002]. *Escartín et al.* [2001] demonstrated that even incipient (9–15%) serpentinization can drastically decrease the overall strength of the lithosphere and promote strain

localization over extended periods of time. This is partly explained by the fact that serpentinites are characterized by a nominally nondilatant mode of brittle deformation where the strain is accommodated through shear cracks within serpentine, while olivine remains undeformed [*Escartín et al.*, 1997].

Talc is a secondary hydrous mineral abundant in the uppermost (few tens of meters) interval of the shear zone associated to oceanic detachment faults, and is one of the weakest phyllosilicate minerals [e.g., *Escartín et al.*, 2008b]. It is stable up to 800°C and ∼5 GPa, and for this reason it is the last phase to break down within subduction zones. It is also extremely weak at low pressure and temperature with a friction coefficient (μ) variable between 0.36 and 0.24 (dry conditions) and ∼0.20 (wet conditions) [*Moore and Lockner*, 2004; *Moore and Rymer*, 2007], although it could also be much lower (i.e., 0.14; *Escartín et al.* [2008b]). The resulting yield stress for talc is < 10% of that of dunite, and ∼20% of that of lizardite (a serpentine mineral), suggesting that talc allows localized failure to occur at lower differential stresses than in other talc-free rocks. Even small amounts (< 10%) of talc are thought to drastically weaken typical oceanic lithosphere rocks [*Escartín et al.*, 2008b]. Furthermore, serpentine and (to an even larger extent) talc enhance pore fluid pressures on the fault surface, further promoting strain localization [*Escartín et al.*, 1997, 2008b].

The widespread occurrence of serpentine-bearing and talc-bearing oceanic detachment faults in modern slow-spreading and ultraslow-spreading oceans may therefore substantially decrease the overall strength of oceanic lithosphere [*Escartín et al.*, 2003; *Schroeder and John*, 2004; *Boschi et al.*, 2006b; *MacLeod et al.*, 2009; *Amiguet et al.*, 2012; *Guillot et al.*, 2015], promoting plastic strain localization upon compression adjacent to spreading ridges, where lithosphere is thin and hot. We, therefore, hypothesize that detachment faults, rather than spreading axes, may efficiently accommodate convergence upon ridge-perpendicular compression, and yield ideal conditions for the nucleation of a new subduction zone parallel and close to (or at) spreading ridges. If correct, this may provide a generic mechanism for subduction initiation along ridges, since detachment faults are likely to form during the (ultra)slow-spreading phase associated with the demise of every ridge immediately prior to their inversion, irrespectively of their initial spreading rate.

3. Subduction Initiation at Oceanic Detachment Faults in the Jurassic Ophiolites of Albania and Greece

3.1. Geochemical Evidence

A ∼500 km long segment of the NW-SE trending ophiolitic belt in the Balkan Peninsula spanning from Albania to Greece (Figure 1) preserves a well-documented compositional subdivision [e.g., *Schmid et al.*, 2008; *Dilek et al.*, 2008; *Robertson*, 2012; *Bortolotti et al.*, 2013]. These ophiolites are remnants of Jurassic oceanic lithosphere that represents the overriding plate of a former intraoceanic subduction zone formed within the western Neotethys Ocean [e.g., *Nicolas et al.*, 1999; *Bortolotti et al.*, 2002, 2004, 2005, 2013; *Bortolotti and Principi*, 2005; *Robertson*, 2012]. High-Ti MORB-affinity crust, indistinguishable from that produced at mid-ocean ridges, dominates in a ∼30 km wide corridor in the west of the ophiolite belt (west Mirdita, Pindos, and Othris; Figure 1), and is locally overlain by very low-Ti (boninitic) lavas; homogeneous SSZ-affinity, low-Ti crust characterizes the eastern domains of the ophiolite belt (east Mirdita, Kukesi, Vourinos; Figure 1) [*Saccani and Photiades*, 2004; *Dilek et al.*, 2008]. This east-west transition from MORB to SSZ crust is gradational, with SSZ-affinity rocks locally overlying MORB-affinity rocks in the western MORB-dominated domains [*Bortolotti et al.*, 2002, 2005, 2013; *Dilek et al.*, 2008; *Robertson*, 2012]. This would suggest that the Jurassic magmatic activity evolved from MORB- to SSZ-signature in this direction, with important implications for the direction of the related subduction system.

Crustal ages inferred from epi-ophiolitic radiolarian cherts indicate that no significant time gap exists between the formation of the MORB (latest Bajocian-early Callovian [*Marcucci et al.*, 1994; *Prela*, 1994; *Prela et al.*, 2000; *Chiari et al.*, 2002, 2004]) and SSZ (latest Bajocian-middle Callovian/early Oxfordian [*Chiari et al.*, 2002, 2003, 2004, 2007; *Marcucci et al.*, 1994; *Marcucci and Prela*, 1996) ophiolites. Similar ages were retrieved with U-Pb ion microprobe (SHRIMP) dating on zircons from plagiogranites and gabbros in the Vourinos (172.9 ± 3.1 and 168.5 ± 2.4 Ma, respectively) and Pindos (171 ± 3 Ma) ophiolites of Greece [*Liati et al.*, 2004].

The emplacement ages of the ophiolite obtained from ^{40}Ar/^{39}Ar geochronology on the metamorphic sole attached at the base of the ophiolite are comparable to the crustal ages (see *Bortolotti et al.* [2013] for a
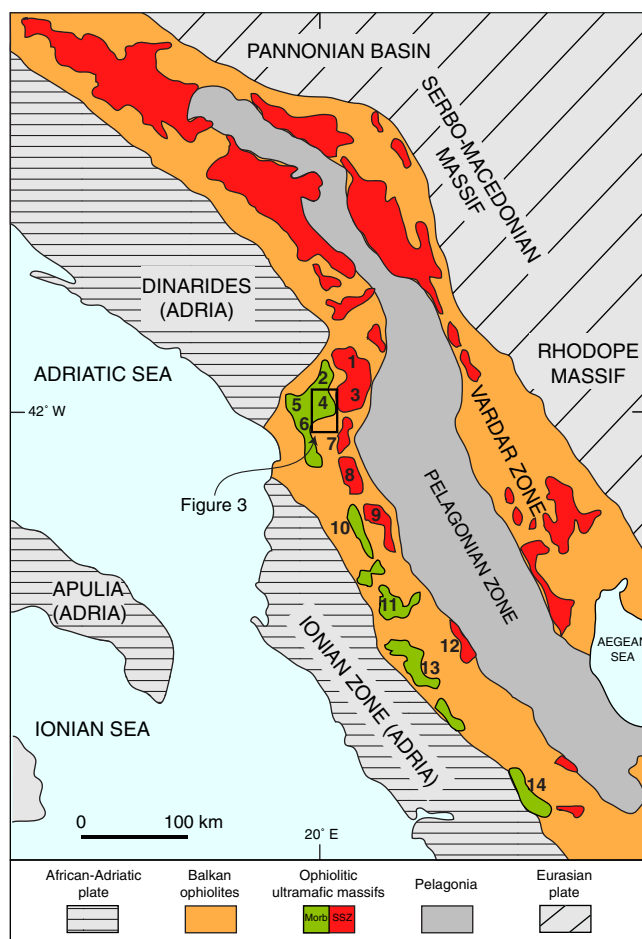
Figure 1. Regional geological map of the central-western Balkan Peninsula, showing the distribution the Jurassic ophiolitic belt and the main geological domains. The ophiolite ultramafic massifs are distinguished into MORB (green) and SSZ (red) affinity, and mark the distinction between western ophiolites characterized by a reduced (3–4 km thick) pseudostratigraphy where a mainly MORB-type crust is associated with a relatively depleted (~10%) [*Bortolotti et al.*, 2013] mantle sequence, and eastern ophiolites showing a complete (8–10 km thick) ophiolite sequence characterized by a subduction-related (SSZ) crust overlying strongly depleted mantle units. Ultramafic massifs are listed as follows: 1, Tropoja; 2, Krrabi; 3, Kukesi; 4, Puka; 5, Gomsiqe; 6, Skenderbeu; 7, Lura; 8, Bulqize; 9, Shebenik; 10, Shpati; 11, Voskopoja; 12, Vourinos; 13, Pindos; 14, Othris.

comprehensive review). In the western MORB ophiolites of Albania, the ages of the metamorphic sole range between 157 ± 12 and 171.9 ± 4.1 Ma, while in the eastern SSZ ophiolites they vary between 153.6 ± 3.4 and 189.4 ± 4 Ma [*Dimo-Lahitte et al.*, 2001]. The western MORB-type ophiolite in the Othris area has a metamorphic sole dated at 169 ± 4 Ma [*Spray et al.*, 1984], while the metamorphic soles from the SSZ-affinity ophiolites in the east show ages of 173 ± 3 [*Roddick et al.*, 1979] to 172 ± 3 Ma [*Spray and Roddik*, 1980] in the Vourinos area, and 171 ± 4 [*Spray et al.*, 1984] in the Pindos area.

The available ages, therefore, do not allow reliable determination of the initial direction of emplacement of the ophiolite, nor the initial polarity of the subduction zone. Although still debated (see *Robertson* [2012] and *Bortolotti et al.* [2013] for comprehensive reviews), the simplest configuration that has been proposed to explain the east-west compositional change of the crust of the Balkan ophiolites requires an east-dipping (below Eurasia) subduction zone formed in the middle Jurassic parallel and close to the active Neotethyan spreading ridge, with an initial (Early Cretaceous) westward emplacement of the ophiolites onto the underthrusting passive margin of Adria [*Beccaluva et al.*, 1994, 2005; *Saccani et al.*, 2004; *Bortolotti et al.*, 2013; *Tremblay et al.*, 2015]. This scenario is supported by (i) kinematic reconstructions of the Alpine-Carpathian-Dinaridic orogenic system [*van Hinsbergen et al.*, 2005; *Schmid et al.*, 2008], (ii) a consistent dominance of westward shear sense indicators (associated with the ophiolite emplacement) in the metamorphic sole attached at the base of the Albanian ophiolite [*Carosi et al.*, 1996; *Bortolotti et al.*, 2005; *Gaggero et al.*, 2009], (iii) top-to-west structural polarity of obduction-related deformation [*Tremblay et al.*, 2015]; and (iv) stratigraphic relationships with syn-obduction and post obduction sedimentary cover sediments of Adria and the ophiolite [*Scherreiks et al.*, 2014]. In contrast, eastward shear sense indicators from the eastern ophiolites of Albania [e.g., *Dilek et al.*, 2008; *Meshi et al.*, 2010] are more scattered, and likely resulting from late stage Alpine tectonics, as suggested by *Bortolotti et al.* [2013]. Further south, the ophiolites of Othris, Pindos, and Vourinos of Greece show more complex patterns suggesting an early eastward intraoceanic emplacement (hence associated to a west-dipping subduction), followed by a westward continental obduction over Adria [*Robertson*, 2012]. A consistent eastward subduction zone cannot, however, be excluded based on the available data.
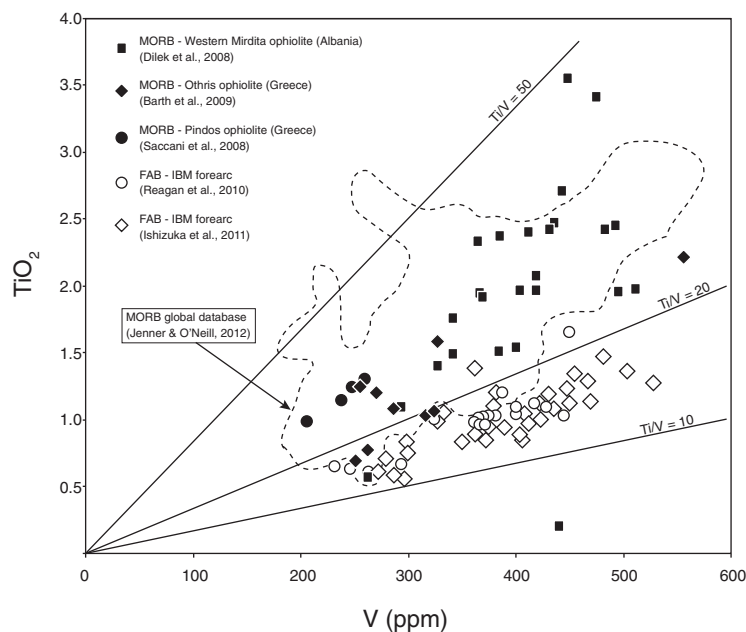
Figure 2. TiO$_2$/V plot for the MORB-type rocks from the western Mirdita (n = 26; data from *Dilek et al.* [2008]), Pindos (n = 9; data from *Barth and Gluhak* [2009]), and Othris (n = 4; data from *Saccani et al.* [2004]), compared with forearc basalts (FAB) from the Izu-Bonin-Mariana (IBM) forearc region reported by *Reagan et al.* [2010] (n = 19), and *Ishizuka et al.* [2011] (n = 32). The MORB field (dotted area) is drawn on the basis of the global database from mid-ocean ridge basaltic glass from *Jenner and O'Neill* [2012]. Basalts from the Balkan ophiolites and those from the IBM forearc plot within two distinct regions of the diagram, indicating that, unlike the FABs, the MORB-type ophiolites of the Balkans were not generated during subduction initiation above a down-going slab. Furthermore, the ophiolitic MORBs plot within the typical MORB field, indicating that they were emplaced at a mid-ocean ridge. Lines of constant Ti/V ratio are also shown. Most of the FABs from the IBM system are characterized by Ti/V ratios between 10 and 20, while the ophiolitic MORBs show Ti/V ratios ranging between 20 and 50.

The assumed polarity of subduction strongly affects the interpretation of the tectono-magmatic evolution of the ophiolites, and in particular the nature of the western MORB ophiolites. In a (most likely) east-dipping subduction configuration, the MORB ophiolites may represent either relics of young (i.e., close to the ridge) lithosphere formed at a preexisting Neo-tethyan mid-ocean ridge that became trapped in the forearc above a nascent subduction zone [*Bortolotti et al.*, 2002, 2005, 2013] or, similarly to examples from the Izu-Bonin-Mariana system, early-stage basaltic products of subduction initiation (so-called forearc basalts, or FABs [*Reagan et al.*, 2010]). Compared to modern MORBs produced at mid-ocean ridge settings [*Jenner and O'Neill*, 2012], FABs show a distinctively lower Ti/V ratio variable between 10 and 20 [*Reagan et al.*, 2010; *Ishizuka et al.*, 2011]. Using published geochemical data from the MORBs from the Mirdita [*Dilek et al.*, 2008], Othris [*Barth and Gluhak*, 2009], and Pindos [*Saccani and Photiades*, 2004] ophiolites of Albania and Greece, we show that the western MORB ophiolites of the Balkans are characterized by a range of Ti/V ratios (i.e., 20–50) that is incompatible with that of typical FABs, and falls within the typical MORB field obtained from the global database of *Jenner and O'Neill* [2012] (Figure 2). This indicates that the western MORB ophiolites of Albania and Greece represent relics of lithosphere that formed at a Neotethyan mid-ocean ridge and were subsequently trapped in the forearc upon subduction initiation.

3.2. Kinematics of a Fossil Detachment Fault in the Mirdita Ophiolite of Albania and Its Tectonic Implications

The MORB-affinity western Mirdita ophiolite preserves a fossil oceanic detachment fault and associated oceanic core complex represented by the ultramafic Puka Massif [*Nicolas et al.*, 1999; *Tremblay et al.*, 2009; *Maffione et al.*, 2013] (Figure 3). Paleomagnetic constraints have documented a westerly tilting of the ser-pentinized fault footwall block exposing ultramafic rocks [*Maffione et al.*, 2013], revealing an easterly dip-ping fault plane, and (since detachments always dip toward the ridge axis [e.g., *Smith et al.*, 2006; *MacLeod et al.*, 2009; *Reston and Ranero*, 2011]), a spreading axis that during detachment activity was located to the east of the presently preserved MORB crust (Figure 4). A mid-ocean ridge origin of the MORB western ophiolites and a paleo-spreading axis located to the east of these units, requires that the east-dipping Juras-sic subduction nucleated off-axis, parallel to and at few tens of kilometers (i.e., no less than the width of the MORB sliver of the western domain) west of the preexisting Neotethyan spreading center.

Considering the slow-spreading character of the Neotethys in the area where these ophiolites were formed [e.g., *Nicolas et al.*, 1999; *Maffione et al.*, 2013], it is very likely that the structure that accommodated subduc-tion, at least in the Mirdita area, was a relatively young detachment fault located close to the active ridge
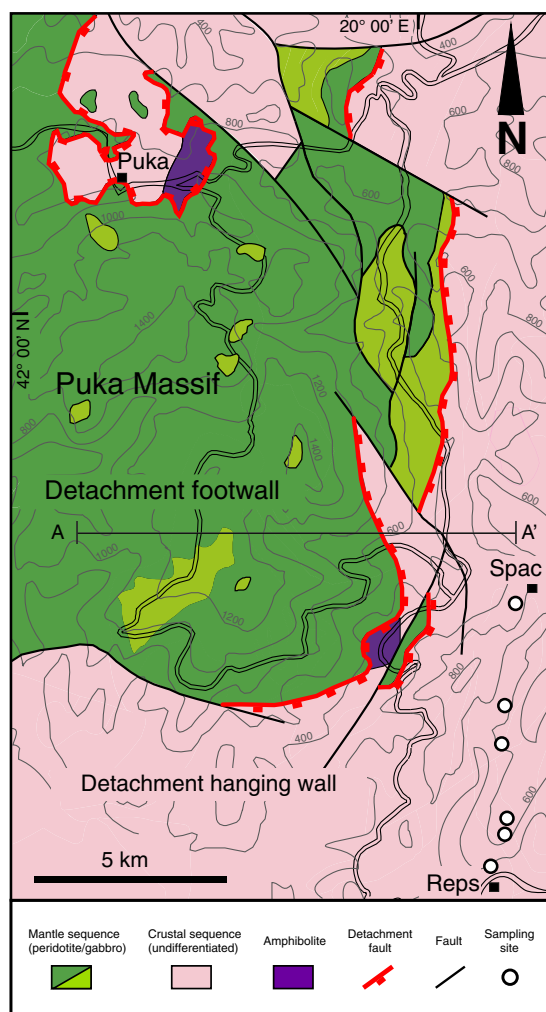
Figure 3. Geological and structural map of the ultramafic Puka Massif in the MORB-affinity western Mirdita ophiolite (see Figure 1 for location). Mantle rocks are mainly refertilized lherzolites and harzburgites [*Nicolas et al.*, 1999]. This mantle sequence is in tectonic contact with upper crustal units composed of sheeted dykes and volcanic rocks (lava flows and pillow lavas) through an oceanic detachment fault formed during Jurassic ocean spreading and preserved in the ophiolite as a fossil structure [e.g., *Maffione et al.*, 2013]. Accordingly, mantle and crustal units are in footwall and hanging wall positions, respectively. Locally, detachment-related amphibolites occur along the fault at the top of the ultramafic units. Paleomagnetic sampling sites in the sheeted dyke complex exposed to the southeast of the massif, and used for the analysis of the paleo-ridge orientation are shown (white dots). A-A', is the trace of the cross section shown in Figure 4.

but not immediately next to it, since a younger detachment was trapped in the upper plate upon subduction initiation. Subsequent rejuvenation of the magmatic activity in the upper plate, likely at the preserved spreading center, must have occurred that generated SSZ crust (i.e., the present-day eastern ophiolites) immediately east of the trapped slice of Neotethyan MORB crust (i.e., the present-day western ophiolites). The initial SSZ melt products may have interacted with the preserved MORB crust providing the intermediate compositions that are frequently described in the western ophiolites [*Dilek et al.*, 2008; *Barth et al.*, 2008; *Barth and Gluhak*, 2009]. This model is consistent with the similar ages (latest Bajocian-early Bathonian; *Bortolotti et al.*, [2013]) of the MORB and SSZ domains, and can elegantly explain the tectono-magmatic evolution of the Albanian ophiolites.

3.3. The Driving Forces of Subduction Initiation in the Western Neotethys: Constraints From Paleomagnetism and Plate Kinematic Reconstructions

The preservation of an oceanic detachment in presubduction Neotethyan lithosphere of the western Mirdita ophiolites indicates that just prior to subduction initiation, spreading in the western Neotethys was slow or ultraslow [*Maffione et al.*, 2013]. In analogy to modern slow-spreading ridges, these extensional structures were likely widespread in this ocean. Upon forced convergence, subduction initiation along such detachments would, therefore, be highly likely. This process would, however, require far-field forcing (sub)perpendicular to the active spreading ridge shortly before the formation of the ophiolitic crust (i.e., 175–170 Ma). Although a subduction initiation

at or near the preexisting Neotethyan spreading ridge has been previously proposed by several authors to explain the geological evolution of the Balkan ophiolites [e.g., *Bortolotti et al.*, 2002, 2005, 2013; *Robertson*, 2012], no quantitative analyses have so far been carried out to reconstruct the actual geometry of the spreading ridge in the Neotethys. While the general orientation of the spreading ridge is commonly inferred from the overall trend of the sheeted dyke complex, this simple approach has been demonstrated to be unreliable due to the potential occurrence of rotations around dyke-perpendicular (or dyke-oblique) axes [*Allerton and Vine*, 1987].

Here, we reconstruct the initial orientation of the spreading ridge using paleomagnetic analysis of MORB-affinity dykes from the sheeted dyke section of the Mirdita ophiolite, and then compare it to the paleogeography obtained from plate kinematic reconstruction. Primary dyke orientations are calculated from paleomagnetic and field structural data using a net tectonic rotation algorithm [*Allerton and Vine*, 1987; *Morris*
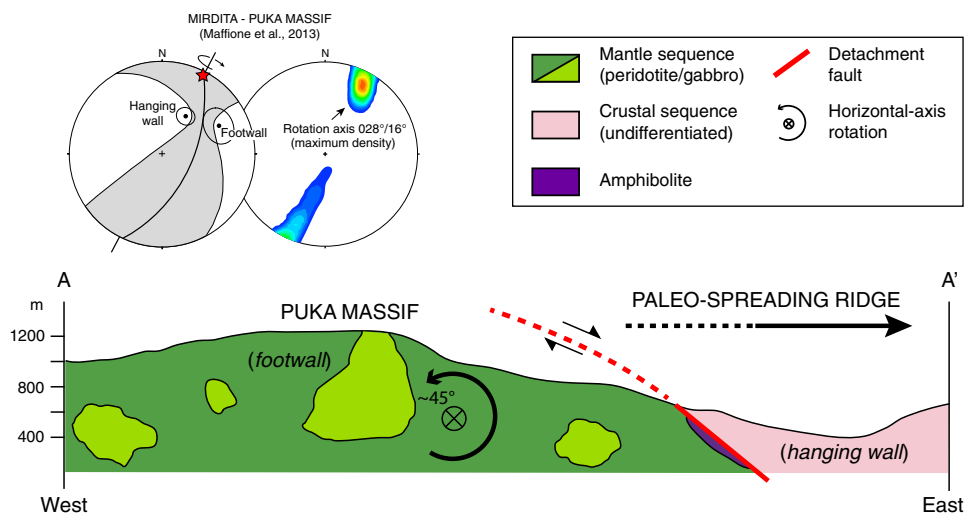
Figure 4. Kinematic analysis of the fossil detachment fault of Puka Massif, and inferred tectonic evolution. Stereonets show the results of the kinematic analysis in *Maffione et al.* [2013] revealing a consistency with a typical "rolling-hinge" mechanism whereby the footwall block of the fault is rotated (by ~45–65°) around ridge-parallel subhorizontal axes (red star). Footwall rotation produces an offset between the footwall and hanging wall magnetization vectors (black dots in the left stereonet). The shaded gray areas are the envelopes of the permissible location of the rotation axis estimated by considering the 95% cones of confidence (ellipses) associated to the paleomagnetic vectors (see supporting information). The solutions of the rotation axis (right stereonet) are displayed as the contour of 5000 permissible solutions obtained from a Monte Carlo simulation. (Bottom) East-west geological cross section (see Figure 3 for location) across the detachment fault. A ~45° of rotation of the ultramafic massif around a subhorizontal ~north-south-trending axis producing a ~westward tilt indicates an ~east-dipping orientation of the detachment fault, according to typical geometries and style of deformation of such structures. Since detachment fault planes normally dip toward the spreading ridge, this geometry indicates an eastward position of the Jurassic paleoridge.

et al., 1998], which is the most reliable tool in sheeted dyke terranes (see supporting information). A mean in situ site magnetization vector (SMV) with declination (D) = 036.2° ± 11.0° and inclination (I) = 47.3° ± 11.4° (k = 77.1; α_{95} = 7.7°) was computed based on primary remanence directions from six sites (39 single remanence directions) within the sheeted dyke complex at the transition zone between MORB and SSZ ophiolite (Figures 3 and 5; supporting information). For the rotation analysis, we adopted a reference magnetization vector (RMV) with D = 000°, and I = 43.0°, based on the unrotated axial geocentric dipole field expected at the paleolatitude of the Mirdita ophiolite in the Jurassic (i.e. 25° N), and in turn based on the APWP and reconstructions of the eastern Mediterranean region. We also assigned a 10° uncertainty in reference inclination, corresponding to the uncertainty in the inclination of the APWP at 170 Ma for the site latitude (i.e. ±6°) [*Torsvik et al.*, 2012], combined with an additional error of ±4° related to the latitudinal width of the Neotethys Ocean at that time [*Schmid et al.*, 2008] (supporting information). We used an in situ mean dyke orientation of 026°/82°E (strike/dip) (α_{95} of dyke poles = 5.3°) determined from 56 measuring points (Figure 5d). To account for the uncertainties associated to the reference direction (RMV), site magnetization vector (SMV), and dyke orientation in the rotation analysis, we followed the approach successfully adopted in other similar settings by *Morris et al.* [1998] (supporting information). A total of 75 permissible solutions obtained from this approach document a mean clockwise rotation of 31.4° (standard deviation = 7.1°) around steeply dipping (azimuth, dip = 224.9°, 70.9°), and an initial dyke strike of 178.7° (standard deviation = 8.5°) (Figure 6).

A reconstructed north-south oriented paleospreading ridge is consistent with previous estimates [*Nicolas et al.*, 1999]. A plate kinematic reconstruction [*Vissers et al.*, 2013; *Gaina et al.*, 2013] in a paleomagnetic reference frame [*Torsvik et al.*, 2012] obtained using GPlates software, demonstrates that this spreading ridge was subparallel to the adjacent passive margins at the time of subduction initiation (Figure 7). In the western Neotethys, subduction initiation coincides with the moment at which the central Atlantic Ocean spreading ridge propagated into the Alpine Tethys [*Vissers et al.*, 2013]. This led to east-west convergence between Adria and the Moesian platform (Eurasia), and created ridge-(sub)perpendicular compression in the western Neotethys (Figure 7). In this paleogeographic configuration, forced subduction initiation along ridge-parallel oceanic detachment faults is thus a plausible scenario.
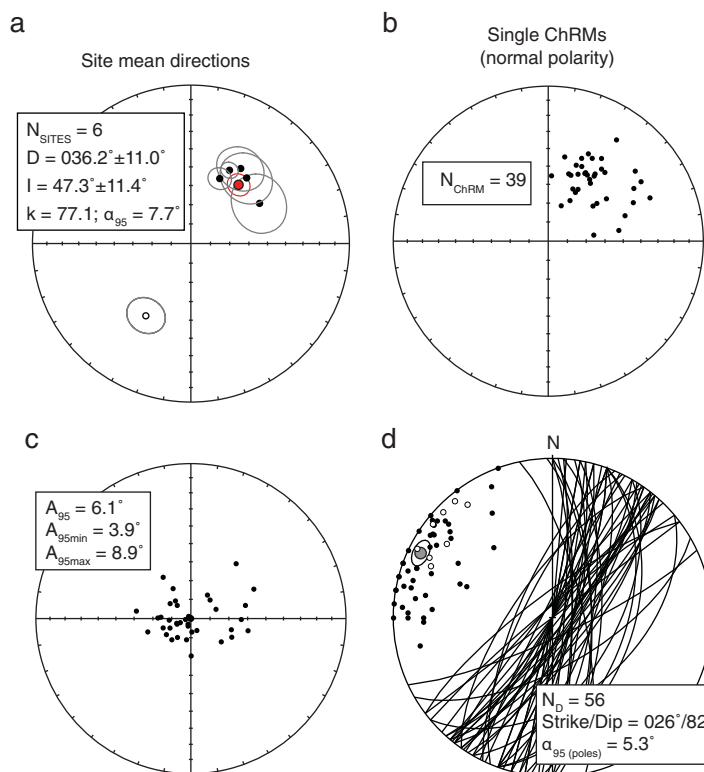
Figure 5. Paleomagnetic analysis of the sheeted dyke section of the Mirdita Ophiolite. (a) Stereographic projection of the in situ site mean paleomagnetic directions and related 95% cones of confidence (dots and ellipses). Solid/open dots correspond to normal/reversed magnetic polarity. N_{SITES}, number of sites used to calculate mean direction (red dot), precision parameter (k), and semiangle of the 95% cone of confidence (α_{95}, red ellipse). (b) Distribution of the 39 single characteristic remanent magnetization directions (N_{ChRM}) from the six sites shown in Figure 5a, and converted to normal polarity. (c) Distribution of the virtual geomagnetic poles (VGPs) corresponding to the characteristic remanent magnetizations (ChRMs) shown in Figure 5b. The semiangle of the 95% cone of confidence around the mean VGP (A_{95}) is between the permissible scatter (i.e., A_{95min}, A_{95max}) expected by paleosecular variation of the geomagnetic field (PSV), and indicates that PSV is adequately represented in this data set (see supporting information). (d) Stereographic projection of the dyke planes and related poles. N_D, number of dykes measured. The semiangle of the 95% cone of confidence (ellipse; α_{95} = 5.3°) around the dyke mean pole (gray dot; 296°/8°) is calculated using Fisherian statistics (see supporting information).

4. Inversion of a Ridge-Detachment System: A Numerical Approach

4.1. Model Setup

From our geological reconstructions, we show that subduction initiated parallel to a mid-ocean ridge, rendering two weakness zones candidates to have localized subduction initiation, oceanic detachments, or the ridge axis: a number of evidence suggests that detachments were preferred over the ridge axis. Because this hypothesis cannot be confirmed from field geological data, we reside to numerical modeling to assess the physical plausibility of the hypothesis that detachments are weaker than ridge axes (Figure 8). Our analysis uses 2-D viscoplastic numerical models carried out with the ELEFANT code, an Arbitrary-Lagrangian-Eulerian thermomechanically coupled Finite Element code, which relies on similar algorithms as its predecessor FANTOM [*Thieulot*, 2011].

Mass, momentum, and energy conservation equations are solved, and materials are tracked by means of markers advecting with the solution obtained on the grid. The size of the computational domain is restricted to 200 × 25 km to increase the resolution on the modeled structures, and is discretized by means of a stretched grid of 1000 × 125 elements. This results in a local resolution of 200 × 130 m near the surface, and 200 × 1083 m at the bottom. We set the temperature at the free surface and bottom to 0°C and 1250°C, respectively. At startup, a fixed temperature of 1250°C is set below 18 km depth, following an approach adopted in previous studies [e.g., *Gerya*, 2010], whereas between the free surface and 18 km depth the temperature follows a half cooling space model characterized by a heat diffusion coefficient $\kappa = 10^{-6}$ m²/s, and an age function of the distance from the spreading axis assuming a steady (full) spreading rate of 2 cm/yr.
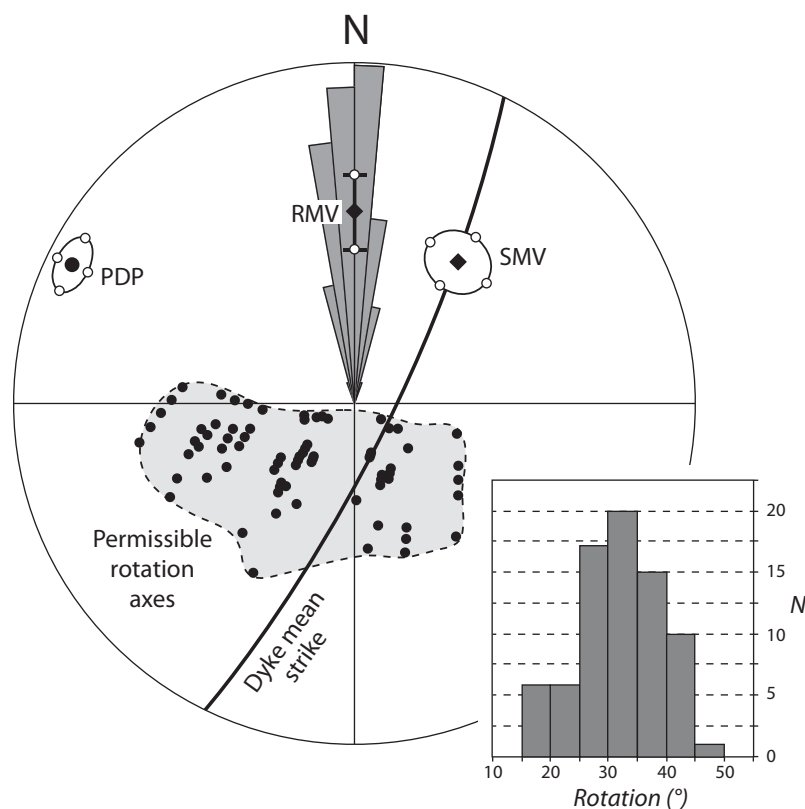
Figure 6. Results of the net tectonic rotation analysis at the sheeted dykes complex of the Mirdita ophiolite. Stereographic projection showing the reference magnetization vector (RMV, declination = 000°; inclination = 43.0° ± 10°), dyke site magnetization vector (SMV, declination = 036.2° ± 11.0°; inclination = 47.3° ± 11.4°), and present mean dyke pole (PDP = 296°/8°), and dyke plane (strike/dip = 026°/82°). Additional points (white dots), besides the mean values, were chosen from each of the three vectors (four for SMV, two for RMV, and four for PDP) to consider the associated errors. A total of 75 permissible rotation axes (black dots and related envelope represented by the shaded gray area), rotation angles (frequency distribution diagram in the inset), and initial dyke orientations (rose diagram) were calculated from the permutations of all the available vectors (five for SMV, five for PDP and three for RMV) (see supporting information).

We perform eight models (supporting information Figures S1, S2, and S3) adopting different boundary conditions dependent on (i) the style (symmetrical versus asymmetrical) and (ii) magnitude (2 and 4 cm/yr) of the velocity field, (iii) the outflux shape of the material at the bottom of the computational domain (flat versus sinusoidal) that compensates the influx velocity due to convergence, (iv) the type and number of lithologies (i.e., with or without uppermost sediments), and (v) the effective viscosity of the serpentine layer along the detachment. All models include a lithospheric discontinuity that geometrically and rheologically resembles modern serpentinized oceanic detachments. Models with higher convergence rate produce a weaker rheology at the spreading ridge since, for a given time interval, fast convergence prevents thermal diffusivity to cool down the system.

The initial setup is described by a 6 km-thick crust (Maryland diabase [*Mackwell et al.*, 1998; *Gray and Pysklywec*, 2012]) that includes (except for Model 6; supporting information Figure S1) a 400 m-thick uppermost layer of sediments [*Buiter et al.*, 2009], mantle peridotites (dry olivine [*Karato and Wu*, 1993]), and a detachment fault cutting lithosphere down to 7 km according to known subsurface geometries [e.g., *Escartín et al.*, 2008a, 2008b; *MacLeod et al.*, 2009; *Reston and Ranero*, 2011]. The intersection of the detachment with the seafloor is set at 15 km from the spreading axis, while at depth the fault is rooted into the axis. The detachment is represented by a 400 m-thick serpentine layer [*Hilairet et al.*, 2007], and exposes a portion of mantle, representing a mature oceanic core complex, at its unroofed footwall (Figure 8).

The serpentinized fault is treated in our models as a viscous layer due to the low viscosity of serpentine and phyllosilicate minerals [e.g., *Boschi et al.*, 2006a, 2006b; *Hilairet et al.*, 2007; *Escartín et al.*, 2008b]. Serpentine is dynamically converted into wet olivine [*Karato and Wu*, 1993] at temperatures above their temperature
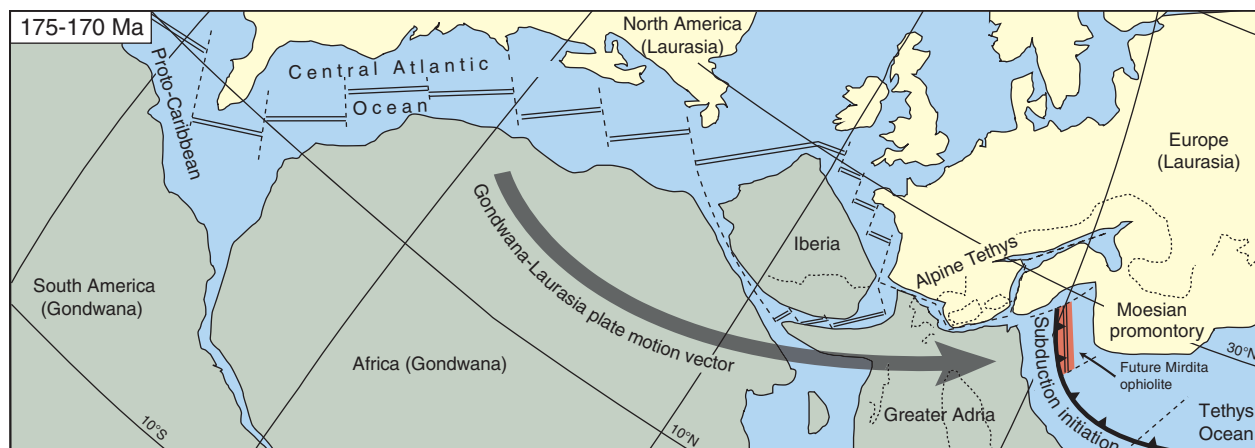
Figure 7. (a) Paleogeographic reconstruction for the Middle Jurassic. Absolute plate position is restored in a paleomagnetic reference frame [*Torsvik et al.*, 2012] using GPlates software. Both the subduction zone and associated spreading center (red area) in the western Neotethys, reconstructed from geological evidence, are subparallel to the adjacent continental margins. Pervasive oceanization (i.e., rifting to drifting) in the central Atlantic, and break-up propagation into the Alpine Tethys may have yielded a ridge-orthogonal (forced) convergence in the northwestern Neotethys that triggered subduction initiation. Double and dotted lines indicate ridge segments and transform faults (and fracture zones), respectively.

stability range (i.e., 200–500°C) during the experiments. All the rheological model parameters are listed in Table 1.

The rheology of the ridge, which is commonly affected by widespread occurrence of high-angle normal faults forming the walls of the spreading valley, is approximated by a trapezium-shaped region of crust (orange area in Figure 1) where the initially accumulated strain is set so that the cohesion and angle of friction of the material are decreased by a strain weakening ratio of five [see *Allken et al.*, 2012], compared to those of the crust. This, results in an extremely weak ridge that may well represent a pervasively fractured (and possibly serpentinized) portion of crust.

To initiate intraoceanic thrusting we apply, after 0.1 Myr thermal re-equilibration of the system (accounting for the time required in geological conditions to switch from spreading to convergence), a constant velocity field producing 40 km shortening.

McKenzie [1977], *Toth and Gurnis* [1998], and *Gurnis et al.* [2004] recognized that the strength of the lithosphere during bending is a critical parameter in the force balance of subduction initiation that has to be taken into account when numerically modeling this process. In slow-spreading oceans, like that considered in our models, however, the mechanical and rheological parameters of the lithosphere are far from homogeneous. In these geological settings, most (80–100%) of plate divergence is accommodated by widespread detachment faulting [*Grimes et al.*, 2008; *Baines et al.*, 2008; *Smith et al.*, 2008; *Escartín et al.*, 2008a, 2008b], which promotes mechanical weakening of the uppermost brittle part of the lithosphere (i.e., the region affected by horizontal stretching during downward bending at the subduction zone). The succession of magmatic and tectonic spreading at a slow-spreading ridge also results in a highly heterogeneous lithosphere characterized by discontinuous and variably thick crust, and upper mantle and lower crust units exposed at the seafloor [*Cannat et al.*, 1995]. More importantly, faulting and mantle exhumation promote water infiltration and pervasive hydrothermal alteration. The main by-products of such processes are ultraweak serpentine minerals and talc [e.g., *Escartín et al.*, 2001, 2008b; *Boschi et al.*, 2006a, 2006b]. Besides allowing failure in these rocks to occur at a lower stress, these minerals reduce the elastic resistance to bending of the lithosphere (i.e., elastic thickness). Based on the curvature of the seafloor at oceanic core complexes, *Smith et al.* [2008] concluded that the elastic thickness at these structures (i.e., < 1 km) is nearly one order of magnitude lower than expected. This suggests that the elasticity of the lithosphere in slow-spreading oceans may be so low that it may not dramatically affect the force balance during subduction initiation. A complete viscoplastic model like that used in this study, may therefore represent a plausible, and realistic approach to model contraction in slow-spreading, detachment fault-dominated ocean basins.
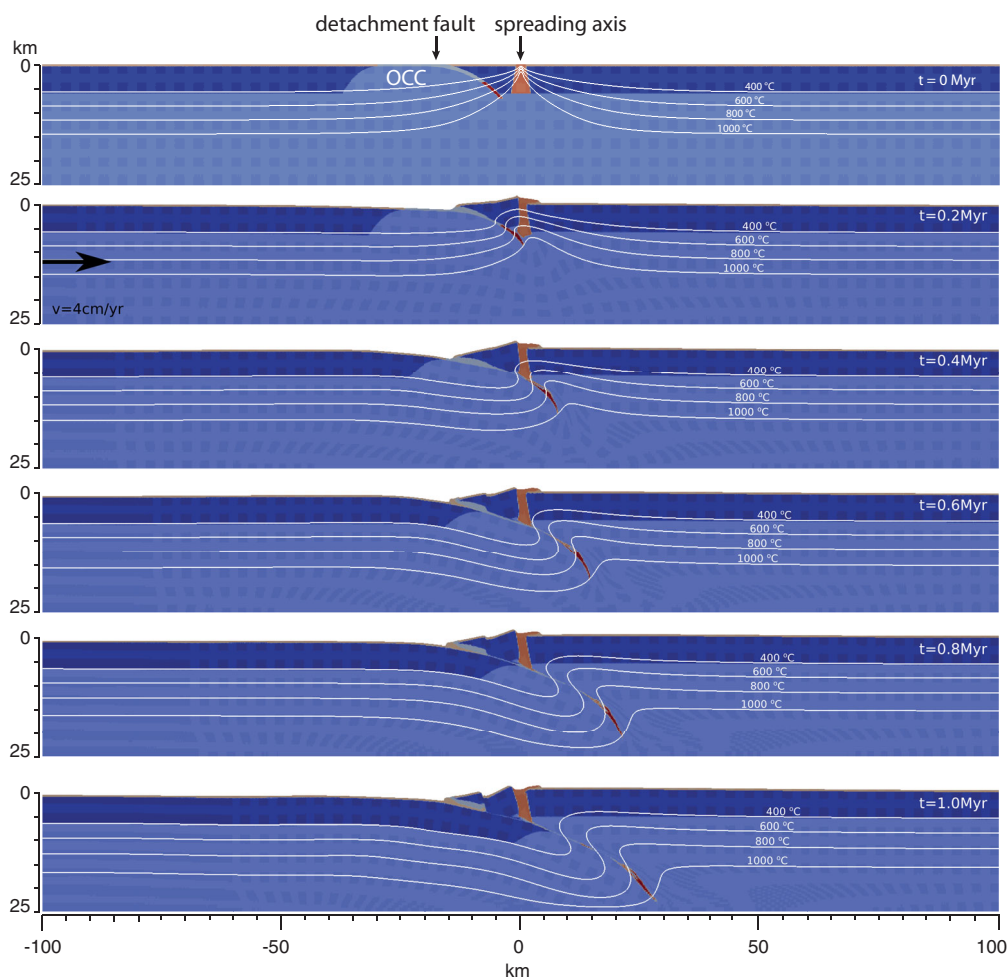
Figure 8. Temporal evolution from 0 to 1 Myr of a detachment-ridge system (Model 2: 4 cm/yr asymmetrical convergence applied to the left side of the computational domain, and a sinusoidal outflux profile (0.5 cm/yr) at the bottom) affected by compression. Materials are as follows: sediments (light orange), crust (dark blue), and mantle (light blue). A detachment fault represented by a 400 m thick layer of serpentine (light green) cuts the crust and part of the upper mantle to a depth of 7 km. Serpentine is converted into wet olivine (red) above 500°C. The portion of crust at the ridge characterized by high strain (enhanced by a factor of five) is shown in orange. OCC, oceanic core complex. Isotherms (white lines) are shown. In the bottom snapshot, the system has experienced 40 km net shortening, which is mainly accommodated by the inversion of the detachment fault (providing the locus of underthrusting), while the ridge only produced minor deformation.

4.2. Results From the Numerical Modeling

Results from our numerical modeling consistently indicate that forced convergence in a ridge-detachment system is largely accommodated by inversion of the detachment fault rather than the ridge axis, i.e., the detachment becomes a thrust (Figure 8). The serpentinized detachment always localizes underthrusting,

Table 1. List of the Main Rheological Parameters Adopted for Materials Used in Our Modeling

	Serpentine	Diabase	Dry Olivine	Sediments	Wet Olivine
Mass density ρ (kg m^{-3})	2650	3000	3300	2400	3300
Thermal expansion α (K^{-1})	4.7×10^{-5}	2.8×10^{-5}	3×10^{-5}	0	3×10^{-5}
Heat capacity c_p (J/mol/K)	5600	750	1200	750	1200
Heat conductivity k (W/m/K)	2.4	2.25	2.25	2.5	2.25
Cohesion c (MPa)	0	10	20	5	20
Angle of friction ϕ	30	15	15	15	15
Material constant A (Pa^{-n}/s)	4.47×10^{-38}	5.04×10^{-28}	2.417×10^{-16}	8.57×10^{-28}	3.9063×10^{-15}
Stress exponent n	3.8	4.7	3.5	4	3
Activation energy Q (kJ/mol)	8.9	485	540	223	430
Activation volume V (cm^3/mol)	3.2	0	20	0	15

even if the spreading axis is very weak, e.g., in Model 2 (supporting information Figure S1). In fact, besides thermal weakening effects at the ridge determined by its spreading rate, we imposed here additional conditions (see previous section) to produce an ultraweak region. Despite this, in most of our models, the ridge only accommodates minor shortening and uplift during convergence and is eventually preserved as a relatively undeformed weak zone in the forearc (Figure 8).

Typical values of effective viscosity of the serpentinized layer result in a fault that is always weaker than the ridge (supporting information Figures S1 and S3b; supporting information). The model using the upper bound for the effective viscosity of the serpentine layer (i.e., $\sim 10^{21}$ Pa.s; supporting information Figure S3a) results in a strong fault, with a rheology comparable to that of the uppermost mantle. In this model, shortening is mainly accommodated at the spreading ridge, which is pervasively deformed until complete disruption (supporting information Figure S3a). Such an extremely strong fault constitutes, however, an unrealistic geologic scenario since both the occurrence of talc and the high fluid pore pressure (parameters that have not been considered in our models) are expected to promote extensive weakening of detachment faults [*Escartín et al.*, 1997, 2008b].

The results of the numerical modeling suggest that the extreme weakness of the detachment fault and its potential to localize deformation under convergence is likely caused by the combined contribution of: (i) low-viscosity serpentine minerals produced by hydrothermal alteration (although talc and other phyllosilicates may as well play a key role in the weakening process [*Escartín et al.*, 1997, 2008b; *MacLeod et al.*, 2002; *Boschi et al.*, 2006b; *Hilairet et al.*, 2007]); (ii) nondilatant (crystal-plastic) deformation style and low strength that characterize serpentine-bearing rocks [*Escartín et al.*, 1997, 2001, 2008b]; (iii) high pore-fluid pressure along the fault interface triggered by phyllosilicates [*Escartín et al.*, 1997]; and (iv) the favorable geometry of the fault, being a lithospheric scale structure, dipping at a low-angle in the upper part of the crust. Not only may these factors aid subduction initiation at detachment faults, but also they are likely to aid the subsequent self-sustained subduction stage [*Hilairet et al.*, 2007].

5. Discussion

Geochemical, structural geological, and paleomagnetic evidence form the Mirdita ophiolite of Albania, indicate that during a Middle Jurassic plate reorganization related to the opening of the Central Atlantic a north-south-striking subduction zone developed within the western Neotethys Ocean parallel to the preexisting ridge (Figure 7). The preservation in the ~ 500 km long ophiolite belt of Albania and Greece of a narrow (i.e., ~ 30 km wide) slice of presubduction initiation Neotethyan MORB lithosphere indicates that subduction initiated not at the ridge axis but few tens of kilometers west of it (Figures 2 and 4). During the early phases of subduction initiation, resumed magmatic activity at the paleoridge in the leading edge of the upper plate determined the accretion of SSZ-affinity crust within Neotethyan MORB-affinity lithosphere. Early Cretaceous emplacement of the forearc onto the continental margin of Adria preserved an ophiolite belt characterized by lateral variation of geochemical signature (i.e., MORB in the west and SSZ in the east see Figure 1).

The region of the Neotethys in which the Albanian ophiolites were accreted was characterized by a so-called detachment-mode of seafloor spreading [*Maffione et al.*, 2013], implying that the ridge was slow-spreading [*Nicolas et al.*, 1999] and detachment faults were likely widespread, as observed in modern slow-spreading oceans like the Atlantic [e.g., *Smith et al.*, 2006, 2008]. Detachment faults form parallel (at or close) to spreading ridges [e.g., *Smith et al.*, 2006, 2008; *Escartín et al.*, 2008a, 2008b; *MacLeod et al.*, 2009] and are extremely weak mainly due to the occurrence of serpentine minerals and talc. The results of our numerical modeling (Figure 8) show that typical serpentinized detachments are always weaker than spreading ridges; these structures, therefore, can yield ideal conditions for the nucleation of new subduction zones upon perpendicular compression at or close to a ridge. It is, therefore, highly likely that the ridge-parallel structure that localized deformation and accommodated plate convergence in the western Neotethys was an ultraweak detachment fault. Whether 2-D numerical models (like those performed in this study) are able or not to reproduce a stable self-sustaining subduction parallel to a spreading ridge remains an outstanding problem [e.g., *Gurnis et al.*, 2004]; the geological evidence from the Balkan ophiolites, however, shows that subduction can start parallel to the spreading ridge, and detachment faults may play a key role in aiding this process.

The main conclusion of our study is that if far-field forces related to e.g., major plate reorganization are at a high angle to an active slow-spreading mid-ocean ridge, a new subduction zone may form parallel and
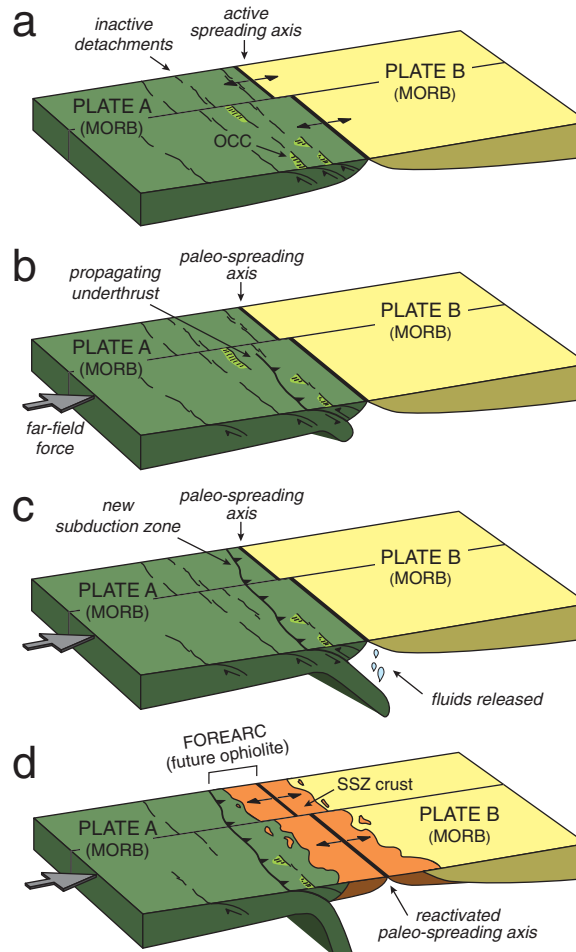
Figure 9. Evolutionary tectonic model of subduction initiation at oceanic detachment faults. (a) Slow-spreading and ultraslow-spreading oceanic lithosphere is pervasively cut by detachment faults, which locally yield oceanic core complexes (OCCs). (b) Detachment faults can localize deformation upon ridge-perpendicular far-field compression, aiding the nucleation of underthrust. (c) Lateral propagation of the initial underthrust results in the formation of a regionally extensive subduction zone. (d) Renewed magmatic activity at the paleo-ridge generates SSZ-type crust. A narrow slice of MORB lithosphere is trapped between the newly formed trench and the paleoridge, and may be locally overlain or intruded by newly formed SSZ melts. The preservation of this MORB sliver may be low due to e.g., subduction erosion processes.

close to it (where lithosphere is hot and thin) along oceanic detachment faults. Owing to the extreme weakness of these faults, mainly due to the occurrence of hydrous minerals such as serpentine and talc, detachments may effectively localize deformation upon compression, allowing failure at very low differential stresses and yielding favorable conditions for the nucleation of a new intraoceanic subduction zone parallel to a preexisting spreading ridge.

If, as observed at the Mirdita ophiolite, subduction initiates along detachments located close to the ridge but not exactly at the spreading axis, the paleoridge remains preserved in the upper plate within a short distance to the new trench (Figure 9). Resumed magmatic activity at the preserved paleoridge during the early phases of subduction initiation produces rocks in the forearc with a geochemical signature that rapidly (i.e., within few million years [*Leng et al.*, 2012]) evolves from MORB (i.e., subduction unrelated) to SSZ and boninitic (i.e., subduction related). A narrow sliver of initial (presubduction initiation) MORB crust may remain trapped between the new trench and the preexisting spreading center (Figure 9). The occurrence (or absence) of this MORB sliver in ophiolite belts may, however, not be diagnostic for this mechanism of subduction initiation at detachment faults, due to its low preservation potential caused by e.g., subduction erosion processes.

The example from the Mirdita ophiolite, where a young (i.e., close to the ridge) rather than the youngest detachment (which was preserved in the upper plate) was reactivated into a subduction zone, suggests that

the potential for these structures to localize subduction initiation is controlled by a combination of factors, including the fault rheology (e.g., the amount of weak minerals like serpentine and talc at the detachment reducing the effective viscosity along the fault during forced compression) and the lithosphere thickness (e.g., detachments far from the ridge, where lithosphere is colder and thicker, do not likely have the required weakness for the subduction initiation process). This suggests that subduction initiation along detachments can only occur within a short distance to the spreading axis; within this region, the detachment with the lowest effective viscosity, controlled by its thermal state and mineralogical assemblage (younger and hotter detachments may be weaker than older and colder ones depending on e.g., the amount and nature of low-viscosity hydrous minerals along the fault), will probably yield the locus of subduction initiation. When sub-duction initiates along off-axis detachments (like in the case of the Mirdita ophiolite), the paleoridge is pre-served as a weakness zone at a short distance from the new trench, facilitating upper plate spreading and emplacement of SSZ melts in a forearc position. Further studies, however, will be needed to fully understand possible causes of forearc spreading and ophiolitic crust accretion in the absence of a preserved paleoridge in the upper plate, e.g., when subduction initiates along detachments at the spreading axis.

While we show that subduction initiation along detachment faults did operate within a specific area of the Neotethys Ocean (Mirdita ophiolite), we can only speculate, based on the extensive occurrence of a narrow belt of Neotethyan MORB crust in the Balkan ophiolites from Albania to Greece (Figure 1), that the same mechanism operated over a larger portion of the Neotethyan spreading ridge. Both ours and previous [e.g., *Hall et al.*, 2003; *Gurnis et al.*, 2004] numerical models for subduction initiation are two-dimensional. Transform-ridge systems, however, are laterally inhomogeneous and the formation of a regionally extensive subduction zone is a three-dimensional problem. Although very long (i.e., 50 km) detachment faults have been documented form the Mid-Atlantic Ridge [*Smith et al.*, 2014], they still represent relatively small struc-tures within first-order ridge segments. Discrete detachments may, therefore, led to the formation of an extensive subduction zone via e.g., (i) lateral propagation of a small subduction zone originally nucleated along a relatively long detachment within a single ridge segment (as suggested in Figure 9), or (ii) simultane-ous nucleation of a subduction zone along multiple detachment faults distributed within adjacent ridge segments.

Key target of future three-dimensional modeling is, therefore, defining (i) the mechanisms whereby discrete detachments along ridge segments can link up upon compression to form a continuous subduction zone; (ii) the mechanisms controlling the formation of single-polarity subduction zones (predominating in mod-ern oceans) even though ridge-detachment systems are symmetric and age relationships across transforms flip across ridges [*van Hinsbergen et al.*, 2015]; (iii) the response of transforms and detachments to oblique convergence (will both invert to develop a segmented subduction zone, or will one predominate over the other?); and (iv) analyzing the potential causes of overriding plate extension intrinsically related to subduc-tion initiation that determine the accretion of SSZ ophiolitic crust.

6. Conclusions

Geological evidence from the Mirdita ophiolite (Albania) and numerical modeling results indicate that intraoc-eanic subduction zones may form not only along transform faults as previously demonstrated, but also along ridge-parallel detachment faults when far-field forces are at high angle to active spreading ridges. Detach-ment faults, which are typically found in slow-spreading oceans, but may also form at fast-spreading ridges just prior to their inversion, are always weaker than spreading axes mainly due to widespread occurrence of serpentine minerals and talc along the fault surface. Upon ridge-perpendicular convergence, detachments can effectively localize deformation, providing favorable mechanical and rheological conditions for subduc-tion to initiate parallel to, and at or near spreading ridges. Subduction initiation at oceanic detachment faults provides a viable explanation for the formation and emplacement of regionally extensive SSZ ophiolitic belts. It enables the nucleation of subduction parallel to spreading ridges, a mechanism otherwise mechanically unlikely, and can ultimately preserve the paleo-ridge (i.e., a large-scale lithospheric weakness) in the forearc. Resumed magmatic activity in the forearc above a subducting slab generates SSZ-affinity crust over a broad area parallel to the trench, which, if obducted onto a continental margin, can remain preserved as an exten-sive ophiolite belt. The formation of a laterally continuous subduction zone across multiple ridge segments by reactivation of discrete detachment fault is an outstanding three-dimensional problem that represents the frontier of current geophysical research on subduction initiation processes.

References

Agard, P., L. Jolivet, B. Vrielynck, E. Burov, and P. Monié (2007), Plate acceleration: The obduction trigger?, *Earth Planet. Sci. Lett.*, *258*, 428–441.

Allerton, S., and F. J. Vine (1987), Spreading structure of the Troodos ophiolite, Cyprus: Some paleomagnetic constraints, *Geology*, *15*, 593–597.

Allken, V., R. S. Huismans, and C. Thieulot (2012), Factors controlling the mode of rift interaction in brittle-ductile coupled systems: A 3D numerical study, *Geochem. Geophys. Geosyst.*, *13*, Q05010, doi:10.1029/2012GC004077.

Amiguet, E., B. Reynard, R. Caracas, B. Van de Moortèle, N. Hilairet, and Y. Wang (2012), Creep of phyllosilicates at the onset of plate tectonics, *Earth Planet. Sci. Lett.*, *345–348*, 142–150.

Andreani, M., J. Escartin, A. Delacour, B. Ildefonse, M. Godard, J. Dyment, A. E. Fallick, and Y. Fouquet (2014), Tectonic structure, lithology, and hydrothermal signature of the rainbow massif (Mid-Atlantic Ridge 36° 14′N), *Geochem. Geophys. Geosyst.*, *15*, 3543–3571, doi:10.1002/2014GC005269.

Bach, W., C. J. Garrido, H. Paulick, J. Harvey, and M. Rosner (2004), Seawater-peridotite interactions: First insights from ODP Leg 209, MAR 15°N, *Geochem. Geophys. Geosyst.*, *5*, Q09F26, doi:10.1029/2004GC000744.

Bach, W., H. Paulick, C. J. Garrido, B. Ildefonse, W. P. Meurer, and S. E. Humphris (2006), Unraveling the sequence of serpentinization reactions: Petrography, mineral chemistry, and petrophysics of serpentinites from MAR 15°N (ODP Leg 209, Site 1274), *Geophys. Res. Lett.*, *33*, L13306, doi:10.1029/2006GL025681.

Baines, A. G., M. J. Cheadle, B. E. John, and J. J. Schwartz (2008), The rate of oceanic detachment faulting at Atlantis Bank, SW Indian Ridge, *Earth Planet. Sci. Lett.*, *273*, 105–114.

Barth, M. G., and T. M. Gluhak (2009), Geochemistry and tectonic setting of mafic rocks from the Othris Ophiolite, Greece, *Contrib. Mineral. Petrol.*, *157*, 23–40.

Barth, M. G., P. R. D. Mason, G. R. Davies, and M. R. Drury (2008), The Othris Ophiolite, Greece: A snapshot of subduction initiation at a mid-ocean ridge, *Lithos*, *100*, 234–254.

Beard, J. S., B. R. Frost, P. Fryer, A. McCaig, R. Searle, B. Ildefonse, P. Zinin, and S. K. Sharma (2009), Onset and progression of serpentinization and magnetite formation in olivine-rich troctolite from IODP Hole U1309D, *J. Petrol.*, *50*, 387–403.

Beccaluva, L., M. Coltorti, I. Premti, E. Saccani., F. Siena, and O. Zeda (1994), Mid-ocean ridge and supra-subduction affinities in ophiolitic belts from Albania, in Beccaluva, L., ed., Special Issue, Albanian ophiolites: State of the art and perspectives, *Ofioliti*, *19*, 77–96.

Beccaluva, L., M. Coltorti, E. Saccani, and F. Siena (2005), Magma generation and crustal accretion as evidenced by supra-subduction ophiolites of the Albanide-Hellenide Subpelagonian zone, *Island Arc*, *14*, 551–563.

Blackman, D. K., J. R. Cann, B. Janssen, and D. K. Smith (1998), Origin of extensional core complexes: Evidence from the Mid-Atlantic Ridge at Atlantis fracture zone, *J. Geophys. Res.*, *103*, 21,315–21,333.

Blackman, D. K., et al. (2011), Drilling constraints on lithospheric accretion and evolution at Atlantis Massif, Mid-Atlantic Ridge 30N, *J. Geophys. Res.*, *116*, B07103, doi:10.1029/2010JB007931.

Bortolotti, V., and G. Principi (2005), Tethyan ophiolites and Pangea break-up, *Island Arc*, *14*, 442–470.

Bortolotti, V., M. Marroni, L. Pandolfi, G. Principi, and E. Saccani (2002), Interaction between mid-ocean ridge and subduction magmatism in Albanian ophiolites, *J. Geol.*, *110*, 561–576.

Bortolotti, V., M. Chiari, M. Marcucci, M. Marroni, L. Pandolfi, G. Principi, and E. Saccani (2004), Comparison among the Albanian and Greek Ophiolites: In search of constraints for the evolution of the Mesozoic Tethys ocean, *Ofioliti*, *29*, 19–35.

Bortolotti, V., M. Marroni, L. Pandolfi, and G. Principi (2005), Mesozoic to tertiary tectonic history of the Mirdita ophiolites, northern Albania, *Island Arc*, *14*, 471–493.

Bortolotti, V., M. Chiari, M. Marroni, L. Pandolfi, G. Principi, and E. Saccani (2013), Geodynamic evolution of ophiolites from Albania and Greece (Dinaric-Hellenic belt): One, two, or more oceanic basins?, *Int. J. Earth Sci.*, *102*, 783–811.

Boschi, C., G. L. Früh-Green, A. Delacour, J. A. Karson, and D. S. Kelley (2006a), Mass transfer and fluid flow during detachment faulting and development of an oceanic core complex, Atlantis Massif (MAR 30°N), *Geochem. Geophys. Geosyst.*, *7*, Q01004, doi:10.1029/2005GC001074.

Boschi, C., G. L. Früh-Green, and J. Escartín (2006b), Occurrence and significance of serpentinite-hosted, talc- and amphibole-rich fault rocks in modern oceanic settings and ophiolite complexes: An overview, *Ofioliti*, *31*, 129–140.

Boschi, C., et al. (2013), Serpentinization of mantle peridotites along an uplifted lithospheric section, mid Atlantic ridge at 11° N, *Lithos*, *178*, 3–23.

Buiter, S. J. H., O. A. Pfiffner, and C. Beaumont (2009), Inversion of extensional sedimentary basins: A numerical evaluation of the localisation of shortening, *Earth Planet. Sci. Lett.*, *288*, 492–504.

Cann, J. R., D. K. Blackman, D. K. Smith, E. McAllister, B. Janssen, S. Mello, E. Avgerinos, A. R. Pascoe, and J. Escartin (1997), Corrugated slip surfaces formed at ridge-transform intersections on the Mid-Atlantic Ridge, *Nature*, *385*, 329–332.

Cannat, M., et al. (1995), Thin crust, ultramafic exposures, and rugged faulting patterns at the Mid-Atlantic Ridge (22°-24°N), *Geology*, *23*, 49–52.

Carosi, R., L. Cortesogno, L. Gaggero, and M. Marroni (1996), Geological and petrological features of the metamorphic sole from the Mirdita nappe, northern Albania, *Ofioliti*, *21*, 21–40.

Casey, J. F., and J. F. Dewey (1984), Initiation of subduction zones along transform and accreting plate boundaries, triple-junction evolution, and forearc spreading centres–implications for ophiolitic geology and obduction, *Geol. Soc. Spec. Publ.*, *13*, 269–290.

Chiari, M., M. Marcucci, and M. Prela (2002), New species of Jurassic radiolarians in the sedimentary cover of ophiolites in the Mirdita area, Albania, *Micropaleontology*, *48*, 61–87.

Chiari, M., V. Bortolotti, M. Marcucci, A. Photiades, and G. Principi (2003), The middle Jurassic siliceous sedimentary cover at the top of the Vourinos ophiolite (Greece), *Ofioliti*, *28*, 95–103.

Chiari, M., M. Marcucci, and M. Prela (2004), Radiolarian assemblages from the Jurassic cherts of Albania: New data, *Ofioliti*, *29*, 95–105.

Chiari, M., V. Bortolotti, M. Marcucci, and G. Principi (2007), New data on the age of the Simoni Melange, Northern Mirdita Ophiolite Nappe, Albania, *Ofioliti*, *32*, 53–56.

Dewey, J. F. (1976), Ophiolite obduction, *Tectonophysics*, *31*, 93–120.

Dewey, J. F., and J. F. Casey (2011), The origin of obducted large-slab ophiolite complexes, in Arc-Continent Collision, Frontiers in Earth Sciences, vol. 15, edited by D. Brown and P. D. Ryan, pp. 431–444, Springer, Berlin Heidelberg.

Dick, H. J. B., J. Lin, and H. Schouten (2003), An ultraslow-spreading class of ocean ridge, *Nature*, *426*, 405–412.

Dilek, Y., H. Furnes, and M. Shallo (2008), Geochemistry of the Jurassic Mirdita Ophiolite (Albania) and the MORB to SSZ evolution of a marginal basin oceanic crust, *Lithos*, *100*(1–4), 174–209.

Dimo-Lahitte, A., P. Monié, and P. Vergély (2001), Metamorphic soles from the Albanian ophiolites: Petrology, ^{40}Ar/^{39}Ar geochronology, and geodynamic evolution, *Tectonics*, *20*, 78–96.

Escartín, J., G. Hirth, and B. Evans (1997), Nondilatant brittle deformation of serpentinites: Implications for Mohr-Coulomb theory and the strength of faults, *J. Geophys. Res.*, *102*, 2897–2913.

Escartín, J., G. Hirth, and B. Evans (2001), Strength of slightly serpentinized peridotites: Implications for the tectonics of oceanic lithosphere, *Geology*, *29*, 1023–1026.

Escartín, J., C. Mével, C. J. MacLeod, and A. M. McCaig (2003), Constraints on deformation conditions and the origin of oceanic detachments: The Mid-Atlantic Ridge core complex at 15°45' N, *Geochem. Geophys. Geosyst.*, *4*, 1067, doi:10.1029/2002GC000472.

Escartín, J., D. K. Smith, J. Cann, H. Schouten, C. H. Langmuir, and S. Escrig (2008a), Central role of detachment faults in accretion of slow-spreading oceanic lithosphere, *Nature*, *455*, 790–794.

Escartin, J., M. Andreani, G. Hirth, and B. Evans (2008b), Relationships between the microstructural evolution and the rheology of talc at elevated pressures and temperatures, *Earth Planet. Sci. Lett.*, *268*, 463–475.

Gaggero, L., M. Marroni, L. Pandolfi, and L. Buzzi (2009), Modeling the oceanic lithosphere obduction: Constraints from the metamorphic sole of Mirdita ophiolites (northern Albania), *Ofioliti*, *34*, 17–42.

Gaina, C., T. H. Torsvik, D. J. J. van Hinsbergen, S. Medvedev, S. C. Werner, and C. Labails (2013), The African plate: A history of oceanic crust accretion and subduction since the Jurassic, *Tectonophysics*, *604*, 4–25.

Garcés, M., and J. S. Gee (2007), Paleomagnetic evidence of large footwall rotations associated with low-angle faults at the Mid-Atlantic Ridge, *Geology*, *35*, 279–282.

Gerya, T. (2010), Dynamical instability produces transform faults at mid-ocean ridges, *Science*, *329*, 1047–1050.

Gray, R., and R. N. Pysklywec (2012), Geodynamic models of mature continental collision: Evolution of an orogen from lithospheric subduction to continental retreat/delamination, *J. Geophys. Res.*, *117*, B03408, doi:10.1029/2011JB008692.

Grimes, C. B., B. E. John, M. J. Cheadle, and J. L. Wooden (2008), Protracted construction of gabbroic crust at a slow spreading ridge: Constraints from 206Pb/238U zircon ages from Atlantis Massif and IODP Hole U1309D (30°N, MAR), *Geochem. Geophys. Geosyst.*, *9*, Q08012, doi:10.1029/2008GC002063.

Guillot, S., S. Schwartz, B. Reynard, P. Agard, and C. Prigent (2015), Tectonic significance of serpentinites, *Tectonophysics*, *646*, 1–19.

Gurnis, M., C. Hall, and L. Lavier (2004), Evolving force balance during incipient subduction, *Geochem. Geophys. Geosyst.*, *5*, Q07001, doi:10.1029/2003GC000681.

Hall, C. E., M. Gurnis, M. Sdrolias, L. L. Lavier, and R. D. Müller (2003), Catastrophic initiation of subduction following forced convergence across fracture zones, *Earth Planet. Sci. Lett.*, *212*, 15–30.

Hilairet, N., B. Reynard, Y. Wang, I. Daniel, S. Merkel, N. Nishiyama, and S. Petitgirard (2007), High-pressure creep of serpentine, interseismic deformation, and initiation of subduction, *Science*, *318*, 1910–1913.

Ildefonse, B., D. K. Blackman, B. E. John, Y. Ohara, D. J. Miller, and C. J. MacLeod (2007), Oceanic core complexes and crustal accretion at slow-spreading ridges, *Geology*, *35*, 623–626.

Ishizuka, O., K. Tani, M. K. Reagan, K. Kanayama, S. Umino, Y. Harigane, I. Sakamoto, Y. Miyajima, M. Yuasa, and D. J. Dunkley (2011), The timescales of subduction initiation and subsequent evolution of an oceanic island arc, *Earth Planet. Sci. Lett.*, *306*, 229–240.

Jenner, F.E., and H. St. C. O'Neill (2012), Analysis of 60 elements in 616 ocean floor basaltic glasses, *Geochem., Geophys., Geosyst.*, *13*, Q02005, doi:10.1029/2011GC004009.

Karato, S. I., and P. Wu (1993), Rheology of the upper mantle: A synthesis, *Science*, *260*, 771–778.

Karson, J. A., G. L. Früh-Green, D. S. Kelley, E. A. Williams, D. R. Yoerger, and M. Jakuba (2006), Detachment shear zone of the Atlantis Massif core complex, Mid-Atlantic Ridge, 30 N, *Geochem. Geophys. Geosyst.*, *7*, Q06016, doi:10.1029/2005GC001109.

Klein, F., W. Bach, N. Jons, T. McCollom, B. Moskowitz, and T. Berquo (2009), Iron partitioning and hydrogen generation during serpentinization of abyssal peridotites from 15°N on the Mid-Atlantic Ridge, *Geochim. Cosmochim. Acta*, *73*, 6868–6893.

Leng, W., and M. Gurnis (2011), Dynamics of subduction initiation with different evolutionary pathways, *Geochem. Geophys. Geosyst.*, *12*, Q12018, doi:10.1029/2011GC003877.

Leng, W., M. Gurnis, and P. Asimow (2012), From basalts to boninites: The geodynamics of volcanic expression during induced subduction initiation, *Lithosphere*, *4*, 511–523.

Liati, A., D. Gebauer, and C. M. Fanning (2004), The age of ophiolitic rocks of the Hellenides (Vourinos, Pindos, Crete): First U-Pb ion microprobe (SHRIMP) zircon ages, *Chem. Geol.*, *207*, 171–188.

Mackwell, S. J., M. E. Zimmerman, and D. L. Kohlstedt (1998), High-temperature deformation of dry diabase with application to tectonics on Venus, *J. Geophys. Res.*, *103*, 975–984.

MacLeod, C. J., et al. (2002), Direct geological evidence for oceanic detachment faulting: The Mid-Atlantic Ridge, 15°45'N, *Geology*, *30*, 879–882.

MacLeod, C. J., R. C. Searle, B. J. Murton, J. F. Casey, C. Mallows, S. C. Unsworth, K. L. Achenbach, and M. Harris (2009), Life cycle of oceanic core complexes, *Earth Planet. Sci. Lett.*, *287*, 333–344.

MacLeod, C. J., J. Carlut, J. Escartín, H. Horen, and A. Morris (2011), Quantitative constraint on footwall rotations at the 15°45'N oceanic core complex, Mid-Atlantic Ridge: Implications for oceanic detachment fault processes, *Geochem. Geophys. Geosyst.*, *12*, Q0AG03, doi:10.1029/2011GC003503.

Maffione, M., A. Morris, and M. W. Anderson (2013), Recognizing detachment-mode seafloor spreading in the deep geological past, *Sci. Rep.*, *3*, 2336, doi:10.1038/srep02336.

Maffione, M., A. Morris, O. Plümper, and D. J. J. van Hinsbergen (2014), Magnetic properties of variably serpentinized peridotites and their implication for the evolution of oceanic core complexes, *Geochem. Geophys. Geosyst.*, *15*, 923–944, doi:10.1002/2013GC004993.

Marcucci, M., and M. Prela (1996), The Lumi i Zi (Puke) section of the Kalur Cherts: Radiolarian assemblages and comparison with other sections in northern Albania, *Ofioliti*, *21*, 71–74.

Marcucci, M., A. Kodra, A. Pirdeni, and T. Gjata (1994), Radiolarian assemblages in the Triassic and Jurassic cherts of Albania, *Ofioliti*, *19*, 105–114.

McKenzie, D. P. (1977), The initiation of trenches: A finite amplitude instability, in Island Arcs, Deep Sea Trenches and Back-Arc Basins, Maurice Ewing Ser., vol. 1, edited by M. Talwani and W. C. Pitman, pp. 57–61, AGU, Washington, D. C.

Meshi, A., F. Boudier, A. Nicolas, and I. Milushi (2010), Structure and tectonics of lower crustal and upper mantle rocks in the Jurassic Mirdita ophiolites, Albania, *Int. Geol. Rev.*, *52*, 117–141.

Mével, C. (2003), Serpentinization of abyssal peridotites at mid-ocean ridges, *C. R. Geosci.*, *335*, 825–852.

Moore, D. E., and D. A. Lockner (2004), Crystallographic controls on the frictional behavior of dry and water-saturated sheet structure minerals, *J. Geophys. Res.*, *109*, B03401, doi:10.1029/2003JB002582.

Moore, D. E., and M. J. Rymer (2007), Talc-bearing serpentinite and the creeping section of San Andreas Fault, *Nature*, *448*, 795–797.

Moores, E. M. (1982), Origin and emplacement of ophiolites, *Rev. Geophys. Space Phys.*, *20*, 735–760.

Morris, A., M. W. Anderson, and A. H. F. Robertson (1998), Multiple tectonic rotations and transform tectonism in an intraoceanic suture zone, SW Cyprus, *Tectonophysics*, *299*, 229–253.

Morris, A., J. S. Gee, N. Pressling, B. E. John, C. J. MacLeod, C. B. Grimes, and R. C. Searle (2009), Footwall rotation in an oceanic core complex quantified using reoriented Integrated Ocean Drilling Program core samples, *Earth Planet. Sci. Lett.*, *287*, 217–228.

Nicolas, A., F. Boudier, and A. Meshi (1999), Slow spreading accretion and mantle denudation in the Mirdita ophiolite (Albania), *J. Geophys. Res.*, *104*, 15,155–15,167.

Pearce, J. A., S. J. Lippard, and S. Roberts (1984), Characteristics and tectonic significance of supra-subduction zone ophiolites, *Geol. Soc. Spec. Publ.*, *16*, 77–94.

Plümper, O., A. Røyne, A. Magrasó, and B. Jamtveit (2012), The interface-scale mechanism of reaction-induced fracturing during serpentinization, *Geology*, *40*, 1103–1106.

Plümper, O., A. Beinlich, W. Bach, E. Janots, and H. Austrheim (2014), Garnets within geode-like serpentinite veins: Implications for element transport, hydrogen production and life-supporting environment formation, *Geochim. Cosmochim. Acta*, *141*, 454–471.

Prela, M. (1994), Mirdita ophiolites project: 1. Radiolarian biostratigraphy of the sedimentary cover of the ophiolites in the Mirdita area (Albania): Initial data, *Ofioliti*, *19*, 279–286.

Prela, M., M. Chiari, and M. Marcucci (2000), Jurassic radiolarian biostratigraphy of the sedimentary cover of ophiolites in the Mirdita area, Albania: New data, *Ofioliti*, *25*, 55–62.

Reagan, M. K., et al. (2010), Fore-arc basalts and subduction initiation in the Izu-Bonin-Mariana system, *Geochem. Geophys. Geosyst.*, *11*, Q03X12, doi:10.1029/2009GC002871.

Reston, T. J., and C. R. Ranero (2011), The 3-D geometry of detachment faulting at mid-ocean ridges, *Geochem. Geophys. Geosyst.*, *12*, Q0AG05, doi:10.1029/2011GC003666.

Robertson, A. H. F. (2012), Late Palaeozoic–Cenozoic tectonic development of Greece and Albania in the context of alternative reconstructions of Tethys in the Eastern Mediterranean region, *Int. Geol. Rev.*, *54*, 373–454.

Roddick, J. C., W. E. Cameron, and A. G. Smith (1979), Permo-Triassic and Jurassic ^{40}Ar/^{39}Ar ages from Greek ophiolites and associated rocks, *Nature*, *279*, 788–790.

Saccani, E., and A. Photiades (2004), Mid-ocean ridge and supra-subduction affinities in the Pindos ophiolites (Greece): Implications for magma genesis in a forearc setting, *Lithos*, *73*, 229–253.

Saccani, E., L. Beccaluva, M. Coltorti, and F. Siena (2004), Petrogenesis and tectono-magmatic significance of the Albanide-Hellenide Subpelagonian ophiolites, *Ofioliti*, *29*, 75–93.

Sauter, D., et al. (2013), Continuous exhumation of mantle-derived rocks at the Southwest Indian Ridge for 11 million years, *Nat. Geosci.*, *6*, 314–320.

Scherreiks, R., Meléndez, G., Boudagher-Fadel, M., Fermeli, G., and Bosence, D., 2014, Stratigraphy and tectonics of a time-transgressive ophiolite obduction onto the eastern margin of the Pelagonian platform from Late Bathonian until Valanginian time, exemplified in northern Evvoia, Greece, *Int. J. Earth Sci.*, *103*, 2191–2216.

Schmid, S. M., D. Bernoulli, B. Fügenschuh, L. Matenco, S. Schefer, R. Schuster, M. Tischler, and K. Ustaszewski (2008), The Alpine-Carpathian-Dinaridic orogenic system: Correlation and evolution of tectonic units, *Swiss J. Geosci.*, *101*, 139–183.

Schroeder, T., B. John, and B. R. Frost (2002), Geologic implications of seawater circulation through peridotite exposed at slow-spreading mid-ocean ridges, *Geology*, *30*, 367–370.

Schroeder, T., and B. E. John (2004), Strain localization on an oceanic detachment fault system, Atlantis Massif, 30N, Mid-Atlantic Ridge, *Geochem. Geophys. Geosyst.*, *5*, Q11007, doi:10.1029/2004GC000728.

Shervais, J. W. (2001), Birth, death, and resurrection: The life cycle of suprasubduction zone ophiolites, *Geochem. Geophys. Geosyst. 2*, 1010, doi:10.1029/2000GC000080.

Smith, D. K., J. R. Cann, and J. Escartín (2006), Widespread active detachment faulting and core complex formation near 13° N on the Mid-Atlantic Ridge, *Nature*, *442*, 440–443.

Smith, D. K., J. Escartín, H. Schouten, and J. R. Cann (2008), Fault rotation and core complex formation: Significant processes in seafloor formation at slow-spreading mid-ocean ridges (Mid-Atlantic Ridge, 13°-15°N), *Geochem. Geophys. Geosyst.*, *9*, Q03003, doi:10.1029/2007GC001699.

Smith, D. K., et al. (2014), Development and evolution of detachment faulting along 50 km of the Mid-Atlantic Ridge near 16.5N, *Geochem. Geophys. Geosyst. 15*, 4692–4711, doi:10.1002/2014GC005563.

Spray, J. G., and J. C. Roddick (1980), Petrology and ^{40}Ar/^{39}Ar geochronology of some Hellenic sub-ophiolitic metamorphic rocks, *Contrib. Mineral. Petrol.*, *72*, 4–5.

Spray, J. G., J. Bebien, D. C. Rex, and J. C. Roddick (1984), Age constraints on the igneous and metamorphic evolution of the Hellenic-Dinaric ophiolites, *Geol. Soc. Spec. Publ.*, *17*, 619–627.

Stern, R. J. (2004), Subduction initiation: Spontaneous and induced, *Earth Planet. Sci. Lett.*, *226*, 275–292.

Stern, R. J., and S. H. Bloomer (1992), Subduction zone infancy: Examples from the Eocene Izu-Bonin-Mariana and Jurassic California arcs, *Geol. Soc. Am. Bull.*, *104*, 1621–1636.

Stern, R. J., M. Reagan, O. Ishizuka, Y. Ohara, and S. Whattam (2012), To understand subduction initiation, study forearc crust: To understand forearc crust, study ophiolites, *Lithosphere*, *4*, 469–483.

Thieulot, C. (2011), FANTOM: Two- and three-dimensional numerical modelling of creeping flows for the solution of geological problems, *Phys. Earth Planet. Int.*, *188*, 47–68.

Torsvik, T. H., et al. (2012), Phanerozoic polar wander, palaeogeography and dynamics, *Earth Sci. Rev.*, *114*, 325–368.

Toth, J., and M. Gurnis (1998), Dynamics of subduction initiation at preexisting fault zones, *J. Geophys. Res.*, *103*, 18,053–18,067.

Tremblay, A., A. Meshi, and J. H. Bédard (2009), Oceanic core complexes and ancient oceanic lithosphere: Insights from Iapetan and Tethyan ophiolites (Canada and Albania), *Tectonophysics*, *473*, 36–52.

Tremblay, A., A. Meshi, T. Deschamps, F. Goulet, and N. Goulet (2015), The Vardar zone as a suture for the Mirdita ophiolites, Albania: Constraints from the structural analysis of the Korabi-Pelagonia zone, *Tectonics*, *34*, 352–375, doi:10.1002/2014TC003807.

Tucholke, B. E., J. Lin, and M. C. Kleinrock (1998), Megamullions and mullion structure defining oceanic metamorphic core complexes on the Mid-Atlantic Ridge, *J. Geophys. Res.*, *103*, 9857–9866.

van Hinsbergen, D. J. J., et al. (2015), Dynamics of intra-oceanic subduction initiation, part 2: supra-subduction zone ophiolite formation and metamorphic sole exhumation in context of absolute plate motions, *Geochem., Geophys. Geosys.*, doi:10.1002/2015GC005745, in press.

van Hinsbergen, D. J. J., E. Hafkenscheid, W. Spakman, J. E. Meulenkamp, and M. J. R. Wortel (2005), Nappe stacking resulting from subduction of oceanic and continental lithosphere below Greece, *Geology*, *33*, 325–328.

Vissers, R. L. M., D. J. J. Van Hinsbergen, P. T. Meijer, and G. B. Piccardo (2013), Kinematics of Jurassic ultra-slow spreading in the piemonte Ligurian ocean, *Earth Planet. Sci. Lett.*, *380*, 138–150.

Whitney, D. L., C. Teyssier, P. Rey, and W. Roger Buck (2013), Continental and oceanic core complexes, *Bull. Geol. Soc. Am.*, *125*, 273–298.